RGNZ/MGPB

The Mechanism of the Kaiser Effect in Phyllite under Indirect Tensile Loading

Rudarsko-geološko-naftni zbornik
(The Mining-Geology-Petroleum Engineering Bulletin)
UDC: 622:2
DOI: 10.17794/rgn.2022.3.2

Preliminary communication

Mohammadmahdi Dinmohammadpour[1]; Majid Nikkhah[2]; Kamran Goshtasbi[3]; Kaveh Ahangari[4]

[1] *Department of Mining Engineering, Science and Research Branch, Islamic Azad University, Tehran, Iran, ORCID http://orcid.org/0000-0003-0573-2510*

[2] *Faculty of Mining, Petroleum and Geophysics Engineering, Shahrood University of Technology, Shahrood, Iran, ORCID http://orcid.org/0000-0002-5961-618X*

[3] *Mining Engineering Department, Tarbiat Modares University, Tehran, Iran, ORCID http://orcid.org/0000-0003-1202-3536*

[4] *Department of Mining Engineering, Science and Research Branch, Islamic Azad University, Tehran, Iran, ORCID http://orcid.org/0000-0001-9462-7303*

Abstract

Determination of in-situ stress serves as an important step in the design and construction of civil and mining projects, among others. Conventional methods of the in-situ stress measurement are time- and cost-intensive. Therefore, the application of low-cost yet rapid methodologies for in-situ stress evaluation has been increasingly regarded by researchers. The Kaiser effect-based acoustic emission method is one of such novel approaches to the in-situ stress evaluation. Not only the point at which the Kaiser effect occurs, but also the mechanism of the Kaiser effect is of paramount importance. In this research, acoustic emission tests were conducted on phyllite rock samples under Brazilian tensile loading to collect a variety of acoustic data, including the amplitude, rise time, count, duration, and energy. Then, the Kaiser effect point was determined using the collected data on acoustic parameters, with its occurrence mechanism investigated. In addition, mathematical transformations were adopted to transform the acoustic signal from the time domain to the frequency domain, where the peak frequency was analyzed. The results of the RA/AF ratio analysis showed that the acoustic emission was sourced from tensile micro-cracks. Moreover, the high level of energy indicated a high intensity of crack formation at the Kaiser effect point. The large number of received hits showed that the count of generated cracks increases abruptly within the range of the Kaiser effect. In addition, the obtained high value of the peak frequency implied that the crack growth rate is high at the Kaiser effect point.

Keywords:
Acoustic emission; Kaiser effect; Peak frequency; Phyllite; Brazilian tensile test

1. Introduction

Engineering design of structures in rocks is impractical without a knowledge of the stress field. Accordingly, during the past 70 years, many attempts have been made to present proper methods for in-situ stress measurement. Acknowledging the high cost and time-intensiveness of the conventional methods (most of which are in-situ methods, including hydraulic fracturing and the overcoring method), the tendency toward the use of low-cost yet fast methods has increased significantly. The acoustic emission method is a low-cost yet rapid methodology for such a purpose. With the help of the acoustic emission method, one can utilize the Kaiser effect to recover the stress memory in such materials as rocks. The Kaiser effect was coined after a German researcher, Joseph Kaiser, when he performed a series of tests on small samples of metal, wood, and sandstone in 1950. Since then, this effect is known under the same title (**Kaiser, 1950**). In the laboratory, the Kaiser effect is induced by subjecting the rock samples to cyclic loading. The Kaiser effect is defined as lack of acoustic parameters prior to achieving the previously applied level of stress to the sample. As seen on **Figure 1**, the acoustic parameters follow increasing trends through the first loading cycle. Following the unloading and upon starting the second loading cycle, the acoustic parameters exhibit no increase until the first-cycle maximum load is reached. As that maximum load is reached, the acoustic parameters increase either abruptly or gradually, indicating what we know as the Kaiser effect. These acoustic parameters include the energy level, count, rise time, amplitude, etc.

For a number of years, the Kaiser effect has been studied for evaluating in-situ stresses although no remarkable success was achieved, with different researchers supporting and criticizing the approach. However, recent research works, especially those performed in Ja-

Corresponding author: Majid Nikkhah
e-mail address: m.nikkhah@shahroodut.ac.ir

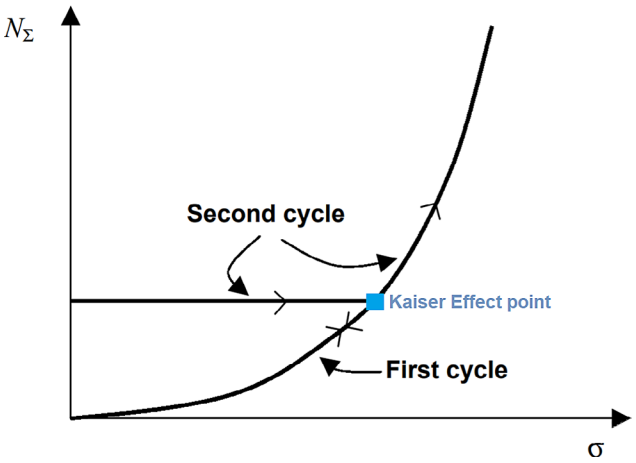

Figure 1: The Kaiser effect point on an AE vs stress graph

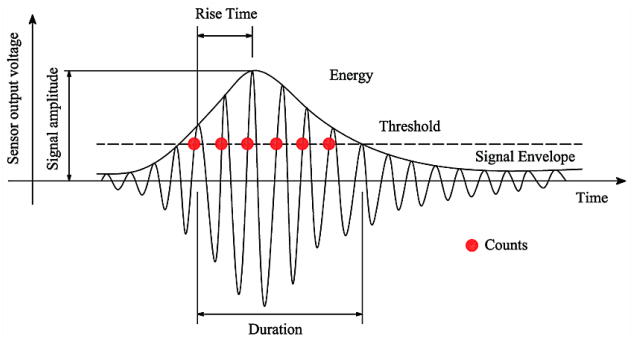

Figure 2: Parameters of acoustic emission signal

pan, Australia, Canada, China, and Belgium, have reported promising findings, highlighting the possibility of stress tensor estimation from different samples of oriented core. Results of these studies have boosted the chances of applying this method in estimation in-situ stress, so that a number of projects have used it to estimate the in-situ stress in practice. The application of AE is divided into three groups: prediction and estimation, monitoring and performance assessment, and detection. The use of AE methods, among other laboratory or in-situ methods, is very fast and accurate, and by only installing specific sensors with data logging equipment, it has been able to process and analyze data online and remotely (**Khoshouei and Bagherpour, 2019**).

Montonon and Hardy conducted a comprehensive review of the studies performed on the Kaiser effect in the field of geological materials. They further investigated the effects of sample medium, test method, multiple stress states, etc. Based on their results, they introduced the Kaiser effect as a simple and low-cost approach to measuring the in-situ stress (**Montoto and Hardy, 1991**). Seto *et al*. investigated the crack propagation in the rock mass using acoustic emission in the laboratory (**Seto et al., 1996**). Seto and Villaescua used the acoustic emission method to evaluate the in-situ stress in a mine premise in Australia, and further compared the results to those of the overcoring method (**Seto and Villaescusa, 1999**). Lavrov stipulated that step-wise loading in three orthogonal direction differs from simultaneous stress application (**Lavrov, 2001**). Tuncay and Ulusay reported research on the balance between the Kaiser effect and the applied prestresses based on the results of in-lab tests (**Tuncay and Ulusay, 2008**). Kent and associates compared the acoustic emission method with other methods and showed that, although the rock type and the level of in-situ stresses compared to the rock strength affect the success rate of the acoustic emission method, this methodology can still provide proper information about the in-situ stresses, especially where brittle deformation is encountered (**Kent et al., 2002**). Yuan and Li presented a theoretical and experimental study on the Kaiser effect in brittle rocks. They suggested that conventional experimental methods for Kaiser effect assessment with the help of acoustic emission must be modified to give more accurate results (**Yuan and Li, 2008**). Li *et al.* conducted an analytic and experimental study on the estimation of in-situ stress using the Kaiser effect. They showed that a large confining pressure in the rock mass can lead to large differences between the Kaiser effect stress obtained from the uniaxial loading tests in the laboratory and actual in-situ stress (**Li et al., 2010**). Nikkhah *et al.* evaluated the Kaiser effect using pattern recognition techniques (**Nikkhah et al., 2011**). Lehtonen *et al.* devised the Kaiser effect to estimate the stress. They reported that stress measurement using the acoustic emission method and the Kaiser effect can render successful when the approach is further supported by key geological information and other stress measurement methods (**Lehtonen et al., 2012**). Hsieh *et al.* showed that the crack formation and propagation process induces some changes in the stress pattern in the proceeding loading cycles when the pre-stress level reaches a higher level than that at the start of dilation in sandstone and ultramafic rocks, so that the acoustic emission commences way before reaching the previous maximum stress and hence no Kaiser effect is observed (**Hsieh et al., 2015**). More recently, Chen *et al.* investigated the occurrence of the Kaiser effect in rocks under tensile loading (**Chen et al., 2018**). Cao *et al.* investigated the effects of static and dynamic loading rates on the rock damage considering the acoustic emission properties (**Cao et al., 2019**). Meng *et al.* presented a study on the Kaiser effect in rocks under Brazilian cyclic loading (**Meng et al., 2019**). Zadsar *et al*. studied fracture mechanisms in anisotropic rocks using the Acoustic Emission method. They showed it was inferred that anisotropy affects the strength and fracture toughness of rock samples (**Zadsar et al., 2020**). Khoshouei *et al.* investigated the acoustic signs of different rock types based on the values of acoustic signal RMS. They suggested RMS values obtained from the acoustic signals can be used in the estimation of rock class and strength properties (**Khoshouei et al., 2020**). Chen *et al.* studied the effect of joint angle on the acoustic emission characteristics of a rock mass (**Chen et al., 2021**). King *et al.* studied acoustic emission waves generated upon rock deformation test using neural networks (**King et al.,**

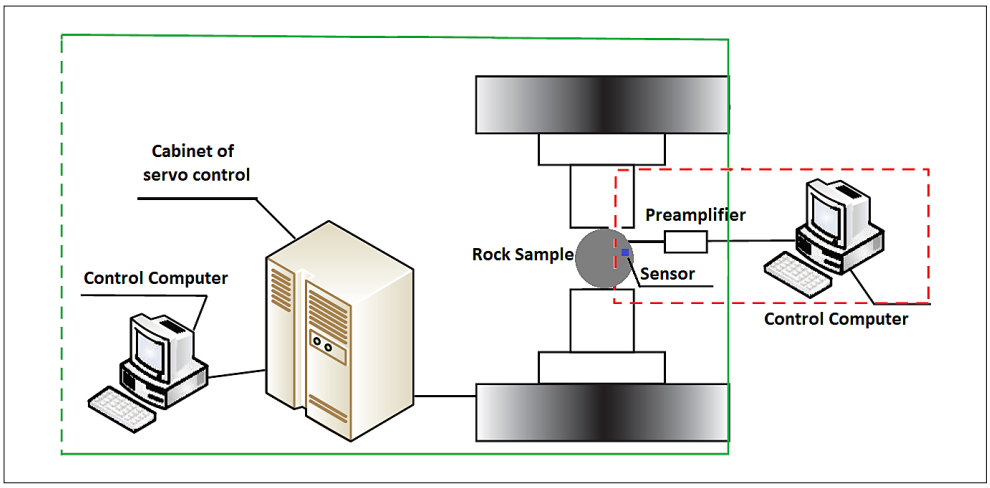

Figure 3: Acoustic emission test system

Table 1: Mechanical properties of Phyllite

name	Uniaxial compressive strength (MPa)	Brazilian tensile strength (MPa)	c (MPa)	Friction angle(°)	Poisson's ratio	Modulus of Elasticity (GPa)
Phyllite	112	12.4	3.3	37.6	0.24	43.57

Table 2: Specification of rock specimens

Sample name	Diameter (mm)	Thickness (mm)	Angle of anisotropy (degree)	Tensile strength (MP)
QP1	53.3	25.9	60	8.1
QP2	53.4	25.4	30	5.8
QP3	53.2	24.2	0	12.4
QP4	53.2	25.3	30	5.8
QP5	53.1	24.2	0	12.4

2021). Li and Xu checked the rock failure mechanism by monitoring the acoustic emission characteristics and micro-seismic activities (**Li and Xu, 2021**). In the same year, Wang *et al.* investigated the failure mechanism and crack propagation in the rock using the acoustic emission method (**Wang et al., 2021**). Zhou *et al.* analyzed the microscopic failure mechanism of rocks subjected to Brazilian dynamic loading based on the acoustic emission characteristics (**Zhou et al., 2021**). Further in 2021, Kharghani *et al.* checked for the effect of anisotropy angle on the Kaiser effect assessment (**Kharghani et al., 2021**). Beltyukov studied the impact of Kaiser effect on the modeling of rock condition in the vicinity of a borehole (**Beltyukov, 2021**). Kunpeng *et al.* investigated the effect of loading angle on the Kaiser effect for sandstone (**Kunpeng et al., 2021**). Fu *et al.* worked on the effect of rise time on Kaiser stress in sandstones (**Fu et al., 2021**).

The mechanism of the Kaiser effect differs in different rocks and under different tests. Generally speaking, in stressed rocks, the acoustic emission can be induced by microcracks and pore clogging, the development of microcracks, fracture formation in grain structure, shear rupture tension, phase conversions, and electric bursts (**Hardy Jr and Leighton, 1984**). From another point of view, in brittle rocks, the acoustic emission is usually associated with microcrack propagation, while it is usually attributed to plastic displacement flow mechanism in formable rocks. It has been further confessed that, in geological materials with their multiple-crystal nature, the acoustic emission can be induced due to micro-scale displacements or macro-scale couplings, grain border shifts, or inter-grain and intra-grain fracture initiation and/or propagation (**Hardy Jr, 2003**).

Based on the theory of acoustic emission testing, a series of the acoustic emission signal parameters (*e.g.* count, rise time, amplitude, persistence time, and peak frequency) are usually used to describe the damage level of respective materials. **Figure 2** depicts the parameters of acoustic emission for a signal.

According to the Japanese standard code of building materials, one can generally classify the sources of acoustic emission under two broad categories, namely tensile and shear cracks. This classification is based on two parameters, namely RA and AF. RA is the ratio of the rise time to peak amplitude of the signal, while average frequency (AF) is defined as the count ratio divided by the persistence time (**Ohtsu and Tomoda, 2007**).

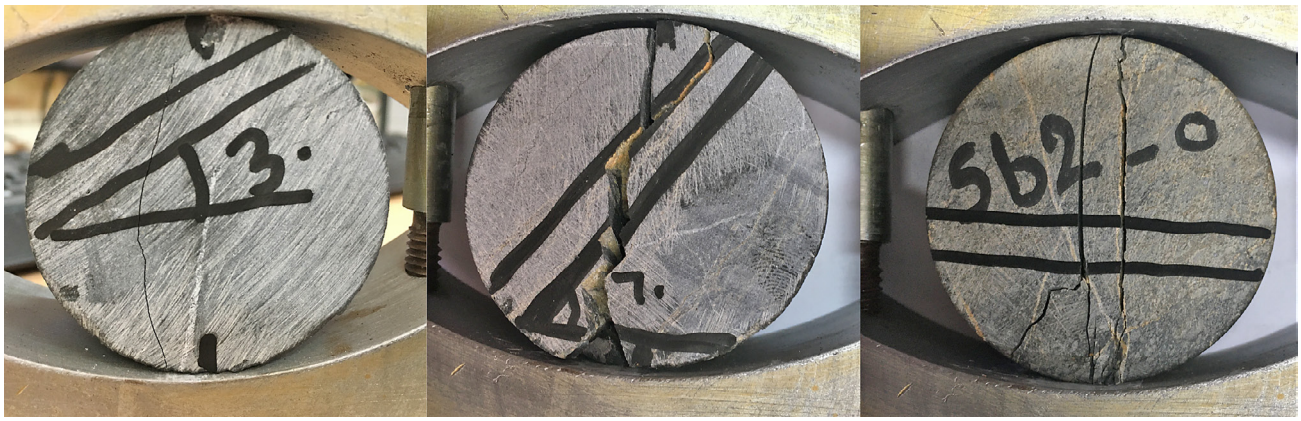

Figure 4: observed failure patterns of samples after the Brazilian tensile strength test

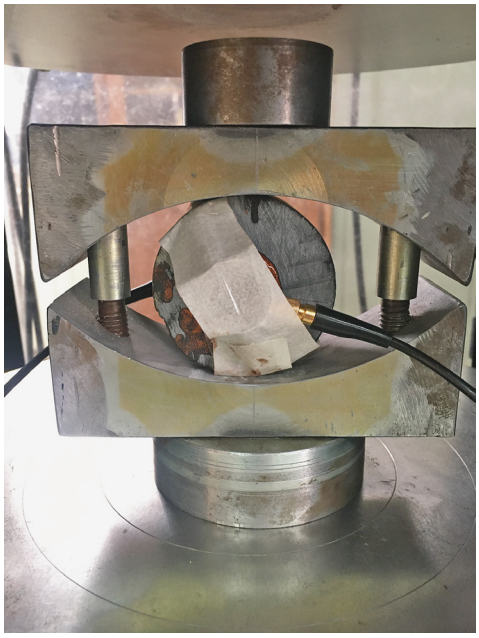

Figure 5: A phyllite sample subjected to Brazilian loading in an acoustic emission test

Other important parameters include energy level and the number hits of the acoustic emission in different periods and what we know as the *b*-value. The energy level is proportional to the cracking intensity, while the number of hits serves as a measure of the count of propagating cracks (**Moradian et al., 2016**). On the other hand, identification of the frequency spectrum of acoustic emission provides some key information regarding the formation of microcracks (**Hou et al., 2021**). Accordingly, one should transform the received signals from the time domain to the frequency domain – a task that can be handled using mathematical transformations.

The *b*-value provides a measure of the count of weak events to strong events. Different fracture configurations produce different acoustic signals with different amplitude and frequency contents. In general, fracture amplitude and size are controlled by the energy released upon crack opening or displacement. Accordingly, small displacements generate low energy levels while large cracks and displacements produce higher energy levels (**Liu, 2000**). Aki proposed an equation based on statistical principles, where he weighed all recorded earthquakes equally to present a new methodology for determining the distribution of independent frequencies and magnitudes of earthquake events (**Sagar et al., 2012**). The method proposed by Aki is one of the methods for calculating *b*-value (**Aki, 1965**). This method is used to study the fracture process in rocks (**Main et al., 1989; Shiotani, 2001**). In the acoustic emission technique, the *b*-value is calculated from Aki's method for independent frequency using Equation (1) (**Kyriazopoulos et al., 2015**). The *b*-value parameter is the logarithmic linear slope of the frequency-amplitude distribution of the acoustic emission. This parameter provides a scale for the distribution of acoustic emission amplitude and is a measure of the relative number of small and large acoustic emissions that indicate local fractures in stressed materials (**Rao and Lakshmi, 2005**).

$$b = \frac{20 \log_{10} e}{< a > - a_c} \tag{1}$$

Where:

$< a >$ – the mean amplitude,

a_c – the threshold amplitude,

e – Euler's number.

The value of $< a >$ can be obtained from Equation 2:

$$< a >= \frac{\Sigma NA}{\Sigma N} \tag{2}$$

Where:

NA – the amplitude of acoustic events,

N – the number of acoustic events.

In this study, a Brazilian test was used to determine the tensile strength of the samples as well as acoustic diffusion tests. Tensile strength measurements for stone samples are done directly and indirectly, of which the Brazilian method is the most famous. These research studies were conducted in three time phases (**Briševac et al., 2015**). Carneiro first conducted research on the

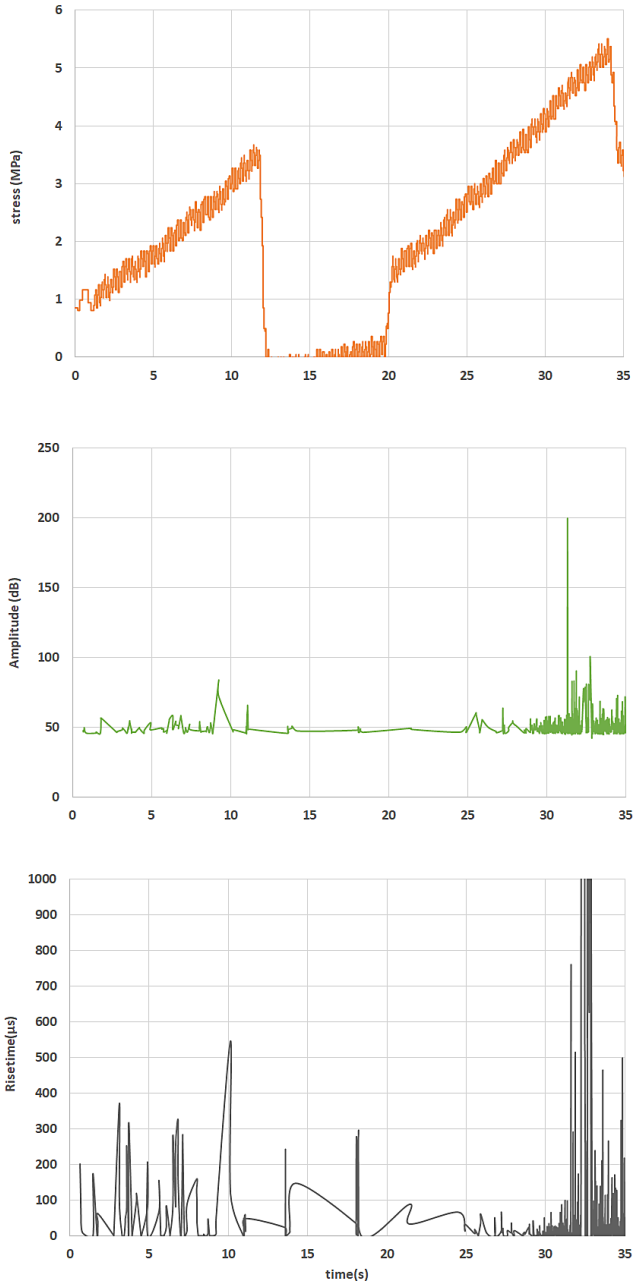

Figure 6: Variations of stress, amplitude, and rise time with time for the sample QP1

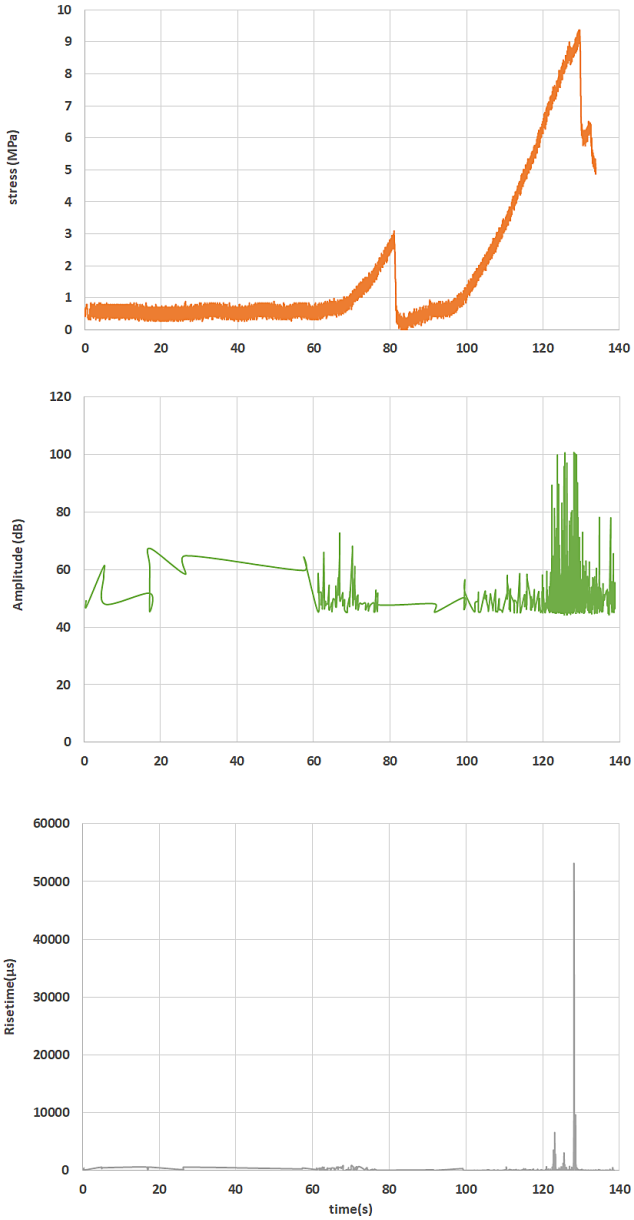

Figure 7: Variations of stress, amplitude, and rise time with time for the sample QP2

Brazilian test (**Carneiro, 1943**). The formula presented is as follows:

$$\sigma_{BTS} = \frac{2F}{\pi.D.t}$$

Where:

σ_{BTS} – indirect tensile strength determined by the Brazilian test (MPa),

F – applied load (kN),

D – diameter of the tested sample (mm),

t – thickness of the tested sample (mm).

Then, in 1978, the International Society of Rock Mechanics presented its proposed method (**ISRM, 1978**). The research studies were conducted in the second phase between 1979 and 1991. The research was conducted in the second phase between 1979 and 1991, the most important of which were the research conducted by Lajtai, Pandey and Singh, and Newman and Bennett (**Lajtai, 1980; Pandey and Singh, 1986; Newman and Bennett, 1990**). In the third phase, researchers such as Lavrov *et al.*, Wang *et al.*, Kazareni, Lin and Wong and Briševac and Kujundžić examined various aspects of the Brazilian test (**Lavrov et al., 2002; Wang et al., 2004; Kazareni, 2013; Li and Wong, 2013; Briševac and Kujundžić, 2015**).

The tested samples are made of phyllite. Phyllite is a foliated metamorphic rock rich in tiny sheets of sericite mica. It presents gradation in a degree of metamorphism ranging between slate and mica schist. The colour varies between black and gray to greenish-gray. The phyllite

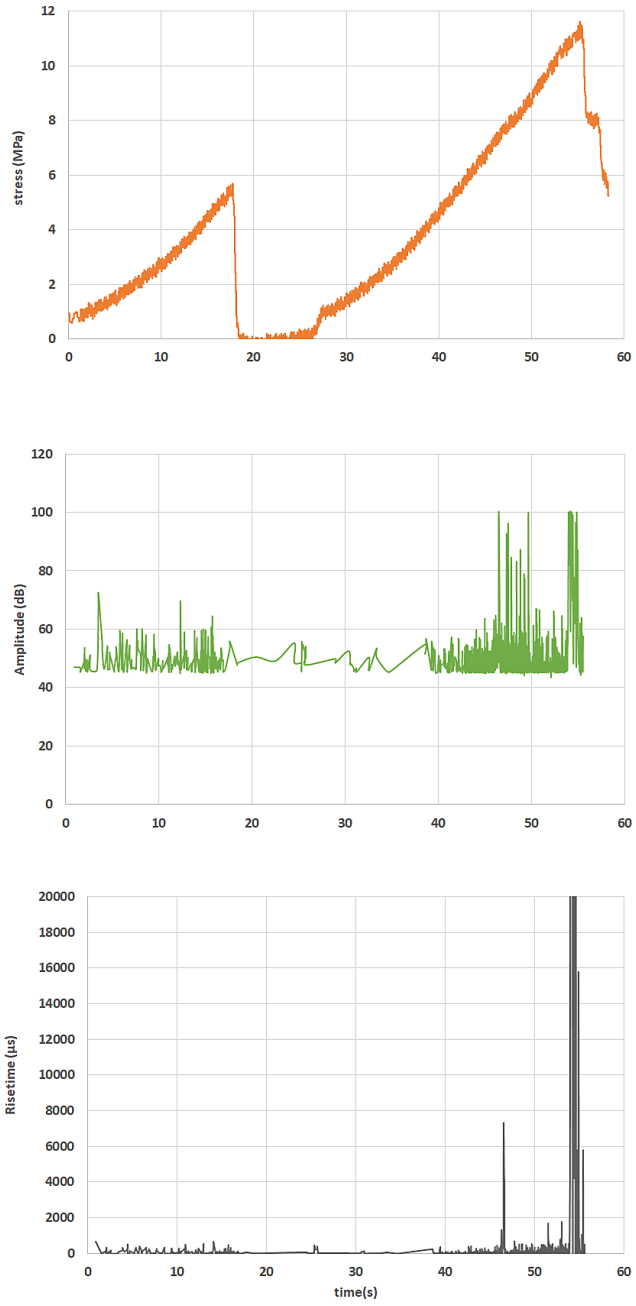

Figure 8: Variations of stress, amplitude, and rise time with time for the sample QP3

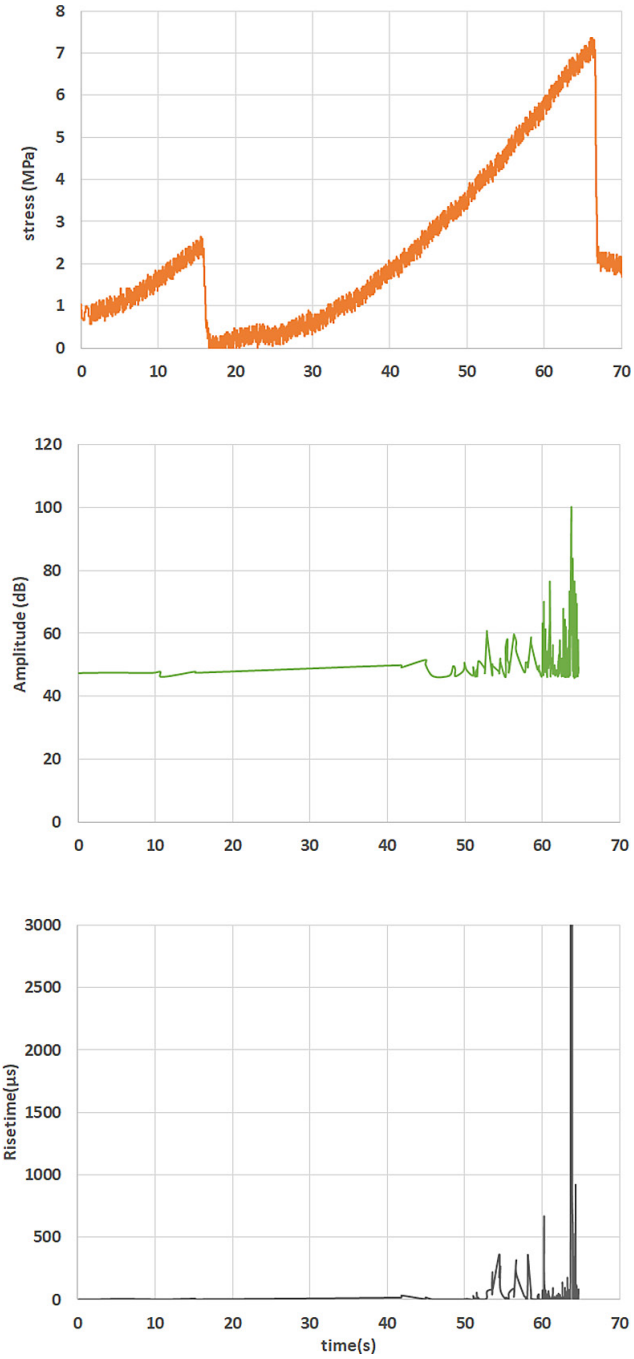

Figure 9: Variations of stress, amplitude, and rise time with time for the sample QP4

forms from pelitic sediments (shale and mudstone) at a slightly higher degree of regional metamorphism from slate (**Haldar, 2020**). Phyllite has good compressive and tensile strength for acoustic tests, which means that it either does not have a very low resistance to failure at low stresses, or it has such high compressive strength that the utilized apparatus does not have enough capability to induce and recover the stress (**Kharghani et al., 2021**).

In this research, we begin by determining the Kaiser effect point through a parametric method followed by investigating all of the mentioned parameters and the mechanism of the Kaiser effect.

2. Methods

In this research, Brazilian loading tests were performed to measure tensile strength of the samples. The ultimate tensile strength of the samples was evaluated to measure the preloading stress, which is usually considered as a percentage of the ultimate strength. The tested rock samples were Phyllite rock, which has anisotropic behaviour, so the tensile strengths obtained were different. We herein performed the Brazilian tests. The testing apparatus is schematically shown in **Figure 3**.

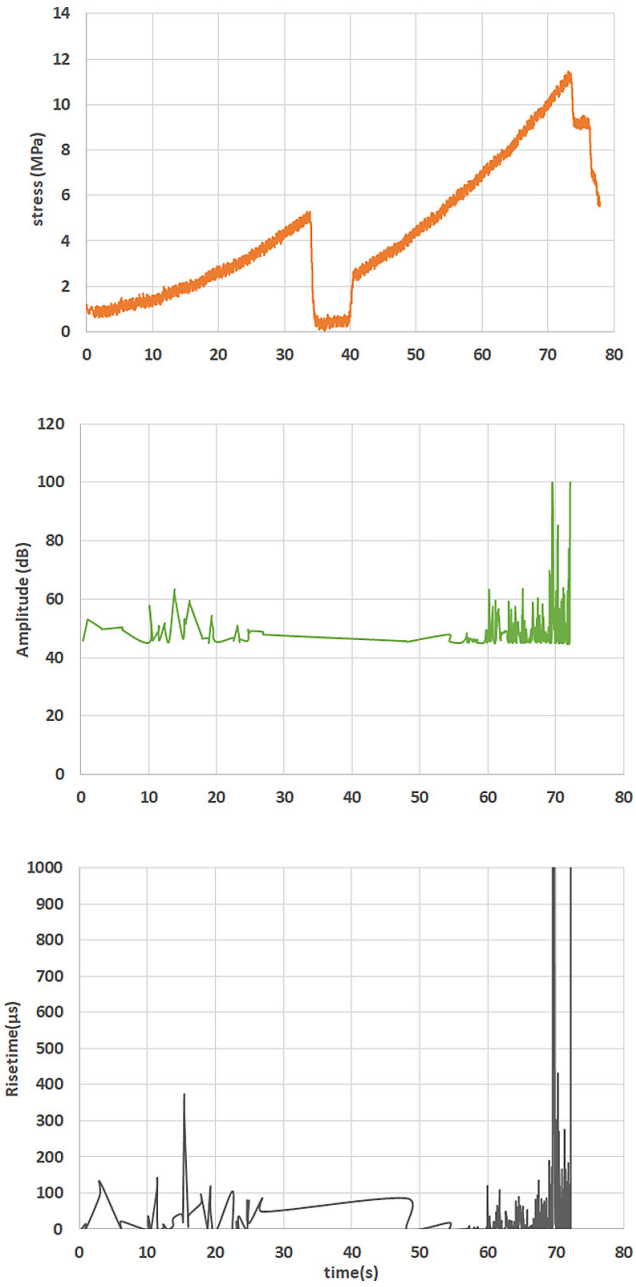

Figure 10: Variations of stress, amplitude, and rise time with time for the sample QP5

Table 1 shows physical and mechanical properties of Phyllite. It should be noted that the experiments were performed according to the ISRM suggested method. Before performing the acoustic emission tests, laboratory tests were performed to determine some of the main mechanical characteristics of the rock sample intended for research.

Rock blocks were collected from the ground that did not experience much stress and the test samples were prepared by core extraction from rock blocks. Samples were collected from western Iran and the Sanandaj-Sirjan Formation. The most important characteristics of rock samples are anisotropic behaviour and brittle rock behaviour. The specification of rock specimens and the results obtained from Brazilian tests are presented in **Table 2**. **Figure 4** shows the observed failure patterns of rock samples after the Brazilian tensile strength test.

The acoustic emission test was herein performed through the following steps:

1. The contact point of the acoustic emission sensor and the rock sample is made of couplant material and the AE sensors are attached to the sample and fixed to the sample with adhesive tape on both sides. Due to the dimensions of the sensors and the rock sample and the appropriate reception of source signals inside the sample, the sensors are embedded in the centre of the disk sample diameter. The sensors were connected to an acoustic data logger. Ensure that the sample surface is thoroughly polished and smooth.
2. Set the data logger configurations including the sampling frequency and other required parameters.
3. Mount the sample inside the Brazilian testing machine. Adjust the jaws of the testing machine on the sample. Use a spacer, if necessary.
4. Start loading and the data logger device simultaneously.

An acoustic emission test begins by subjecting the sample to a first loading cycle (pre-loading). In subsequent experiments, the value of preloading stress was selected at about 70 to 80% of the final strength to create a stress memory in the rock. Next, full unloading is performed and a second loading cycle is triggered immediately until the failure point is reached. In all stages, acoustic data is being collected, for further analyses, through two sensors installed on the disk samples. **Figure 5** shows a sample under Brazilian loading in an acoustic emission test, with the sensor positioning further indicated.

Based on the results of several tests, the threshold was determined at 45 dB. This threshold was set to attenuate the ambient noise and the noise contents associated with the testing machine itself and the sample-machine contacts, not to mention other possible sources of noise.

3. Results and Discussion

In this research, the Kaiser effect point was evaluated using the amplitude and rise time. **Figure 6** shows the plot of stress, amplitude and rise time versus time for the QP1 sample. As indicated on the figure, no increase is observed in neither the amplitude nor the rise time prior to 31.3 s. At this time, however, abrupt increases occurred in the level of acoustic parameters, indicating the occurrence of the Kaiser effect at this time.

Similar to **Figure 6**, **Figure 7** refers to the sample QP2. Considering **Figure 7**, it is evident that the acoustic data remained almost unchanged until 123.6 s, at which time an abrupt increase in the data occurred, indicating the occurrence of the Kaiser effect. **Figure 8** dem-

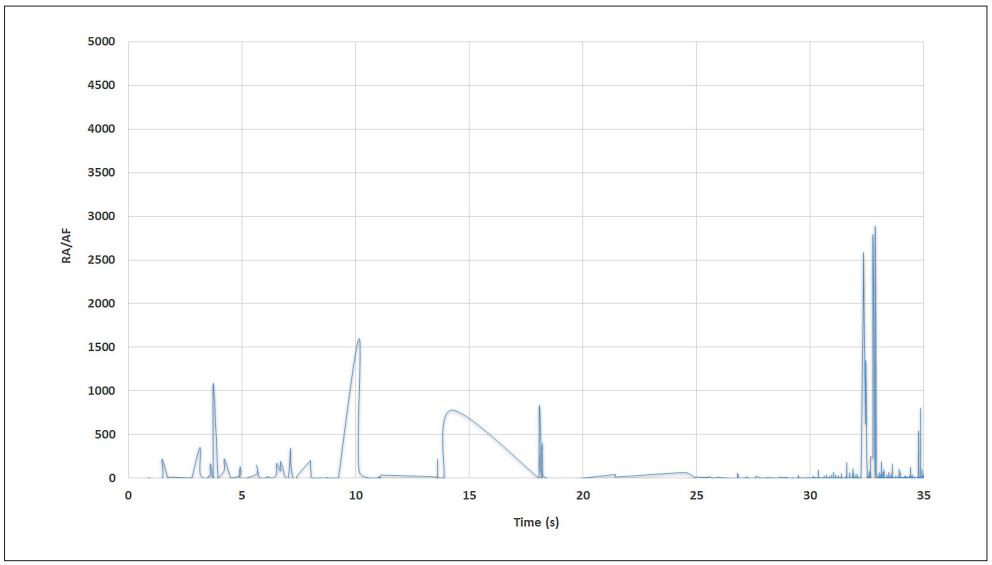

Figure 11: Variations of RA/AF with time for the sample QP1

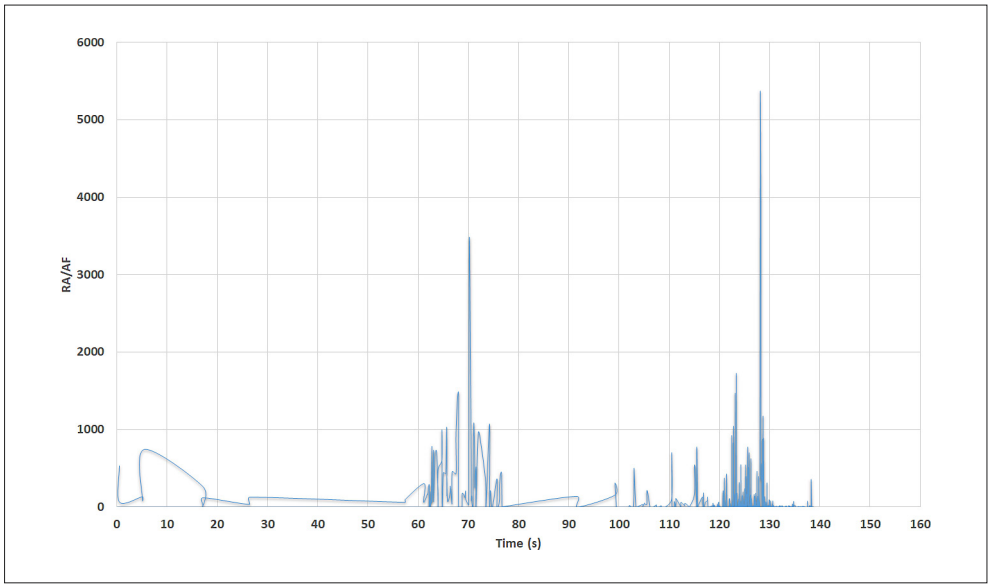

Figure 12: Variations of RA/AF with time for the sample QP2

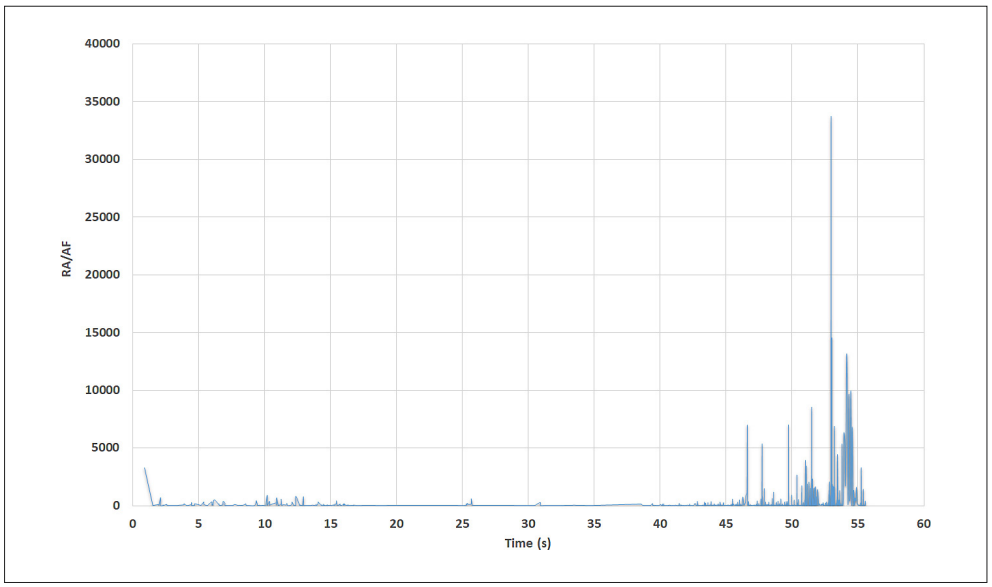

Figure 13: Variations of RA/AF with time for the sample QP3

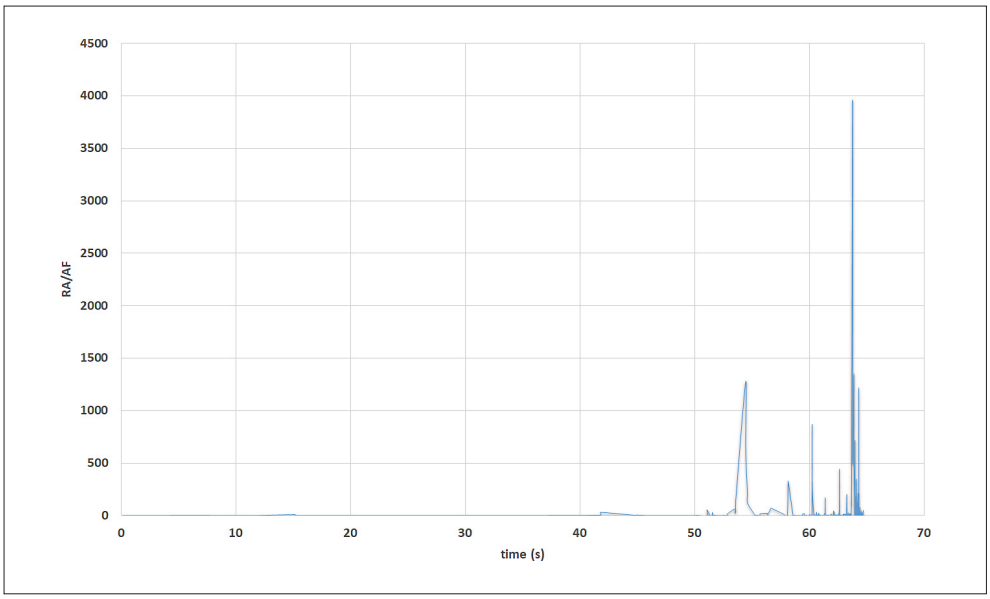

Figure 14: Variations of RA/AF with time for the sample QP4

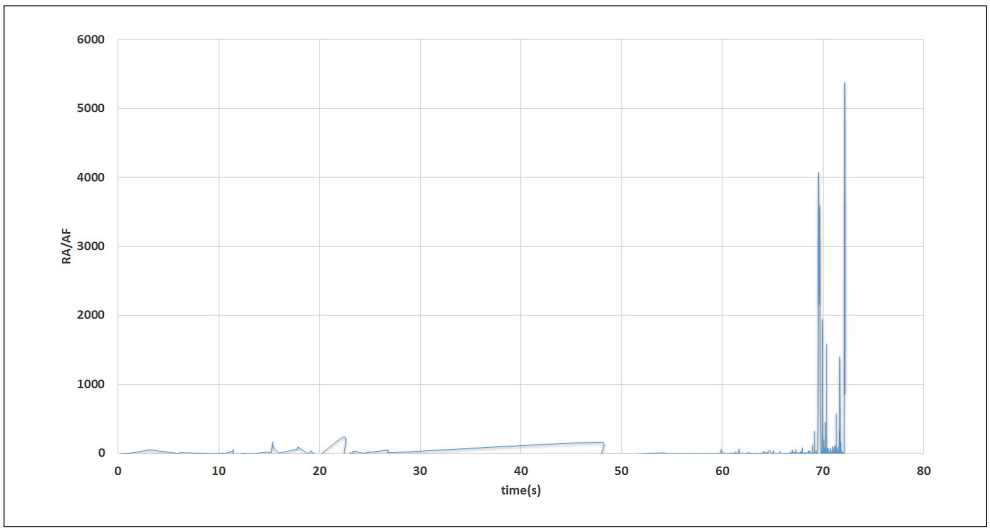

Figure 15: Variations of RA/AF with time for the sample QP5

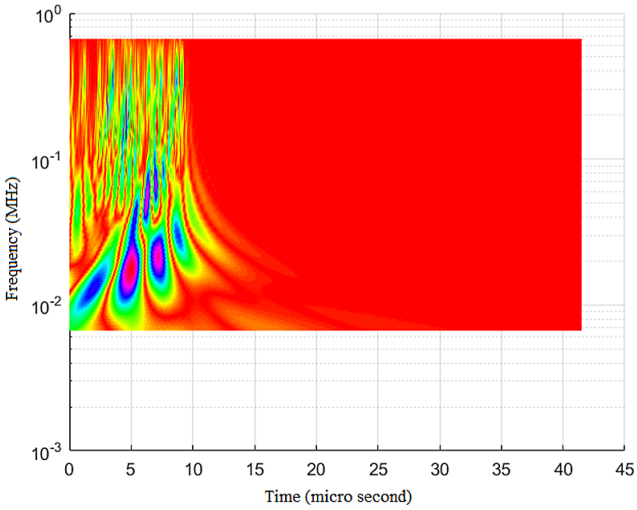

Figure 16: Two-dimensional diagram of peak frequency for hit no. 342 of the Sample QP1

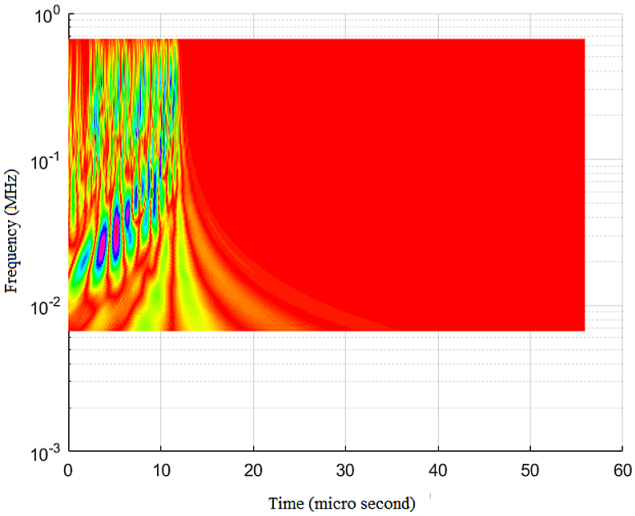

Figure 17: Two-dimensional diagram of peak frequency for hit no. 497 of the Sample QP2

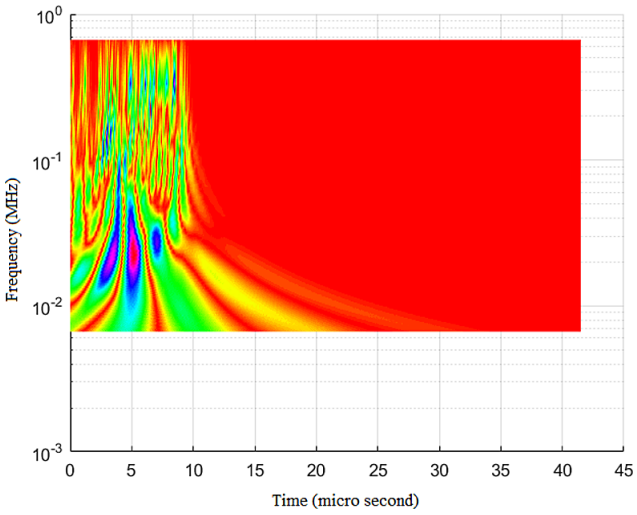

Figure 18: Two-dimensional diagram of peak frequency for hit no. 802 of the Sample QP3

onstrates the plots of applied stress, amplitude, and rise time versus time for the sample QP3. Based on the figure, the Kaiser effect occurred at 46.5 s for this sample. According to **Figure 9** and **10**, the Kaiser effect for samples 4 and 5 occurred in 52.8 and 60 seconds, respectively.

According to the Japanese standard code of building materials, a high RA coupled with a low AF describes acoustic emission events sourced from shear microcracks, while a low RA coupled with a high AF characterizes the acoustic emissions generated upon tensile microcracks (**Ohtsu and Tomoda, 2007**). Therefore, the RA/AF ratio provides a good criterion for characterizing the source of an acoustic emission event. As seen in **Figure 11** (referring to the sample QP1), the value of RA/AF ratio is low at the time of the Kaiser effect (*i.e.* 31.3 s), implying that the effect is a result of some tensile crack formation. The same state is seen in **Figures 12** to

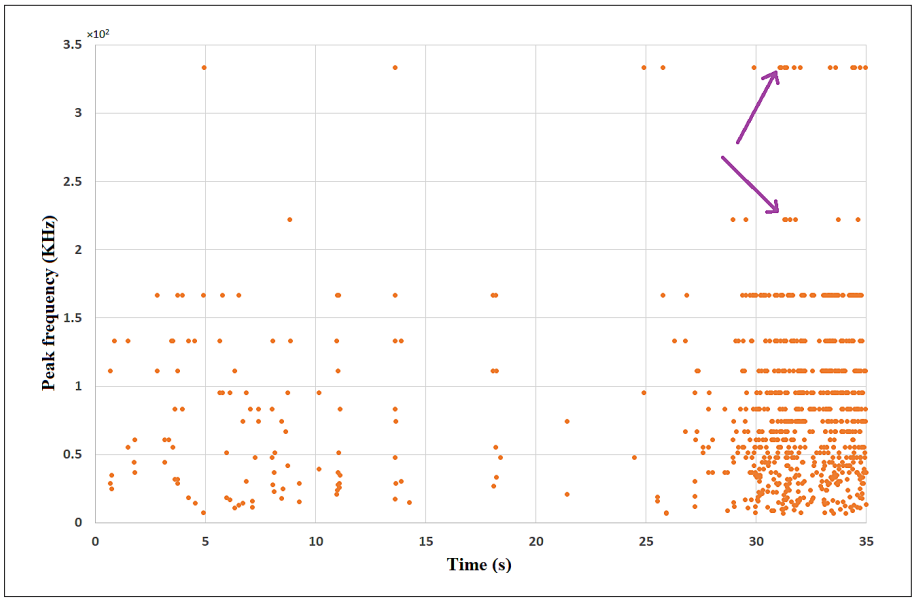

Figure 19: Peak frequencies in all received hits for the sample QP1

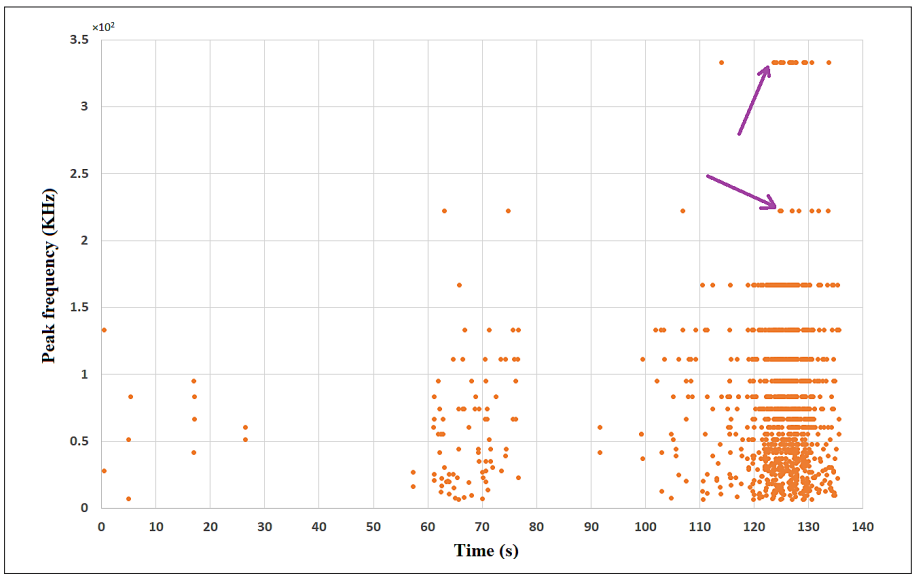

Figure 20: Peak frequencies in all received hits for the sample QP2

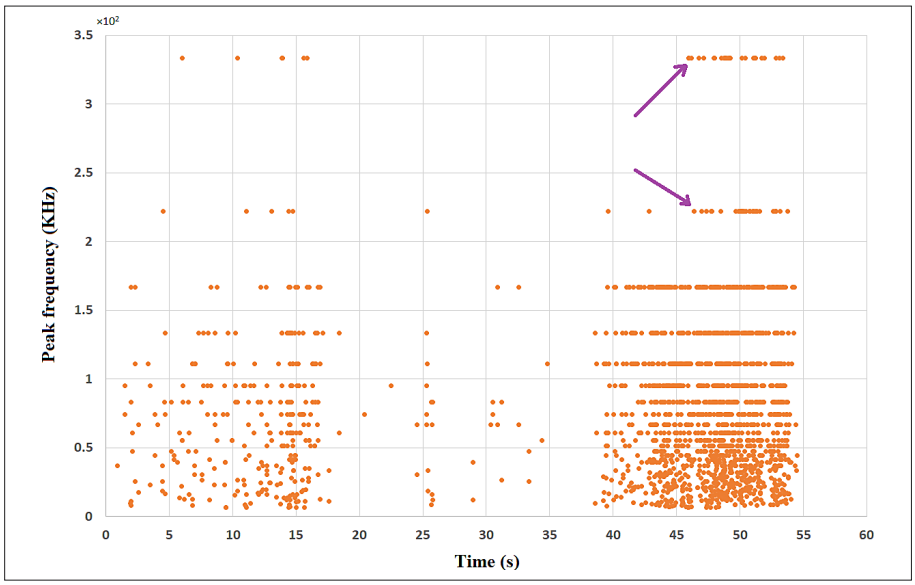

Figure 21: Peak frequencies in all received hits for the sample QP3

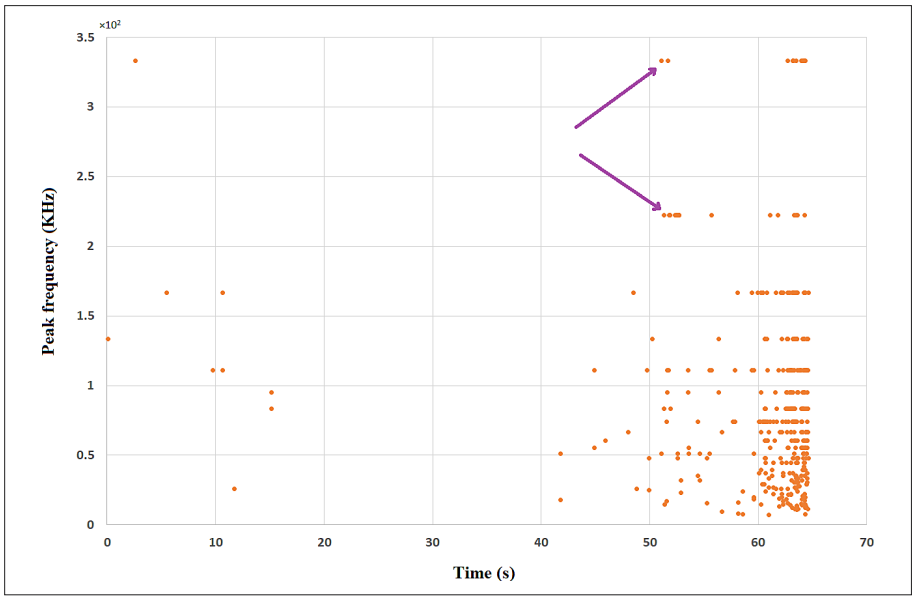

Figure 22: Peak frequencies in all received hits for the sample QP4

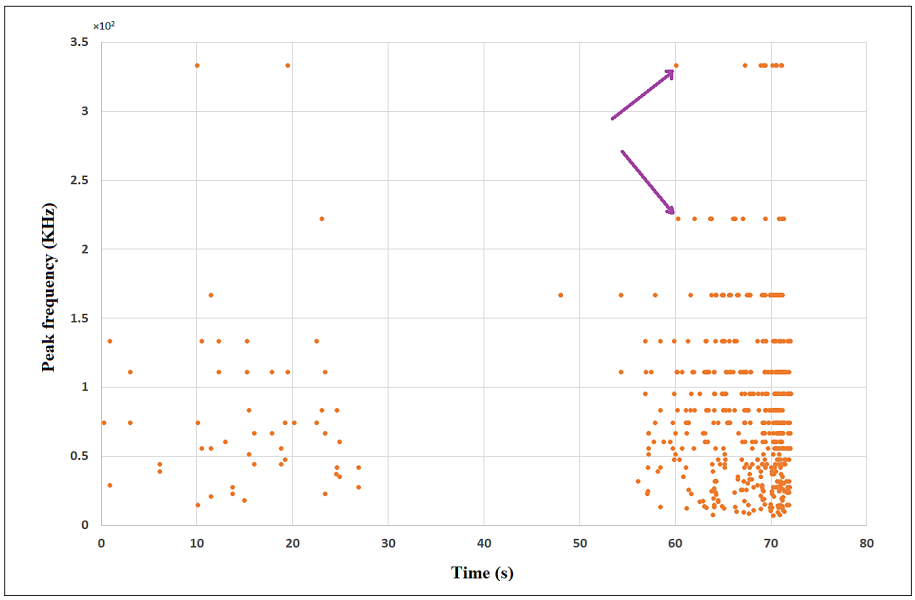

Figure 23: Peak frequencies in all received hits for the sample QP5

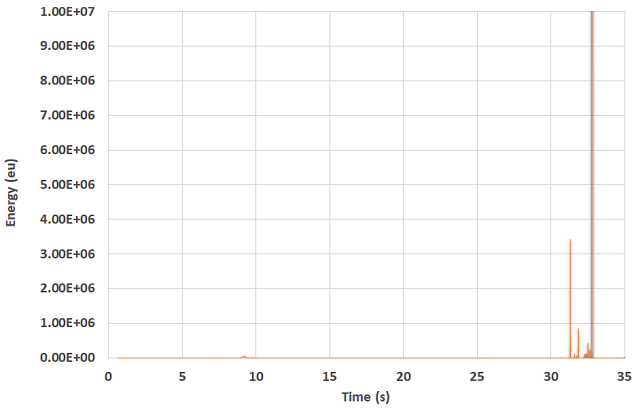

Figure 24: Variations of energy level with time for the sample QP1

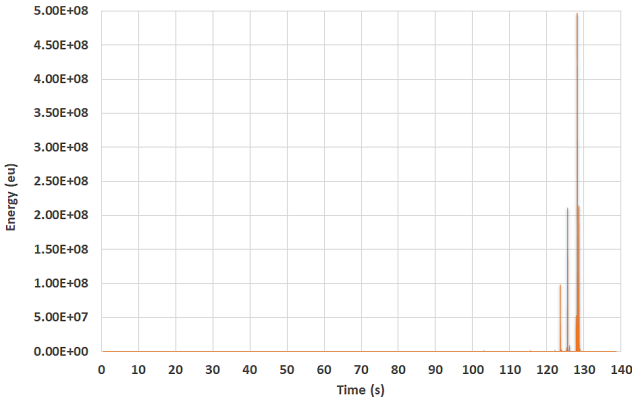

Figure 25: Variations of energy level with time for the sample QP2

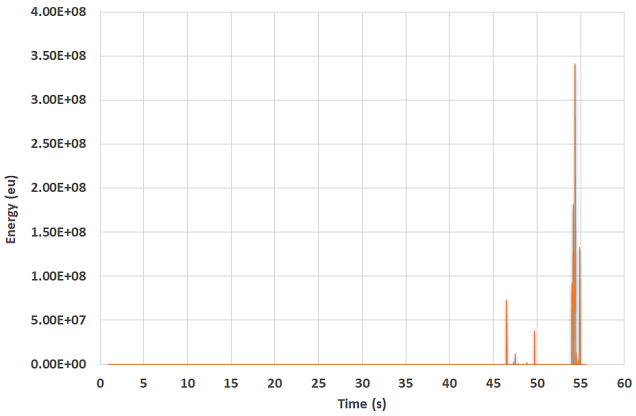

Figure 26: Variations of energy level with time for the sample QP3

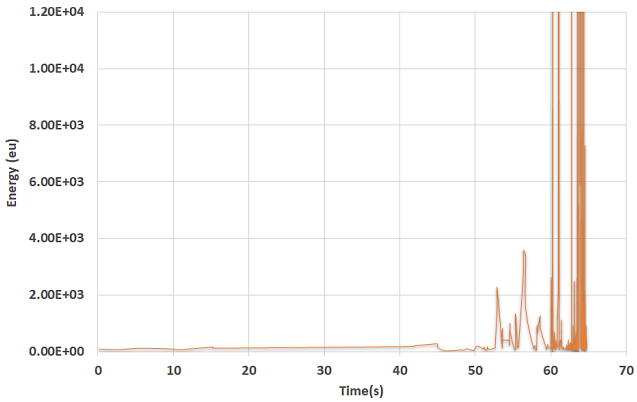

Figure 27: Variations of energy level with time for the sample QP4

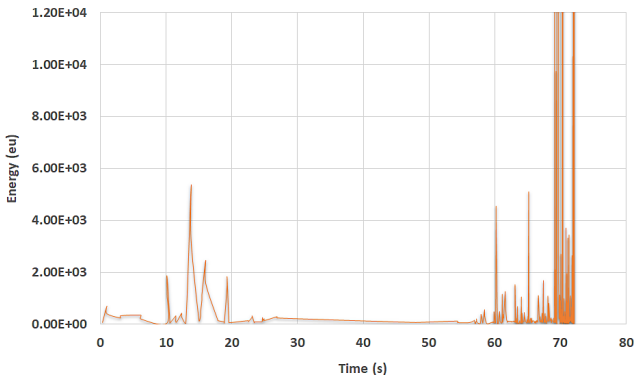

Figure 28: Variations of energy level with time for the sample QP5

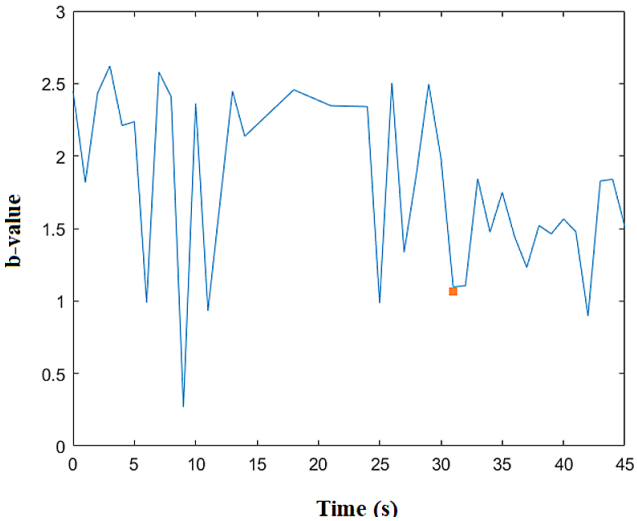

Figure 29: Variations of b-value with time for the sample QP1

15 where the Kaiser effect occurs at 123.6, 46.5, 52.8 and 60 s, respectively, reflecting the dominant contribution of tensile cracks into the Kaiser effect.

The crack pattern from which acoustic emission is originated can be obtained from the characteristics of the distribution of peak frequency of the acoustic emission signals (**Hou et al., 2021**). Peak frequency is a popular parameter in the analysis of acoustic emission signals. As mentioned earlier, this parameter can be assessed by transforming the signal from the time domain to the frequency domain. Once finished with importing the data from the data logger into the software, mathematical transformations were applied to different hits associated with the samples. The peak frequency was considered as a required parameter for analyzing the mechanism of the Kaiser effect, with the relevant data extracted. **Figures 16** through **18** demonstrate examples of the obtained peak frequency diagrams for the samples QP1 through

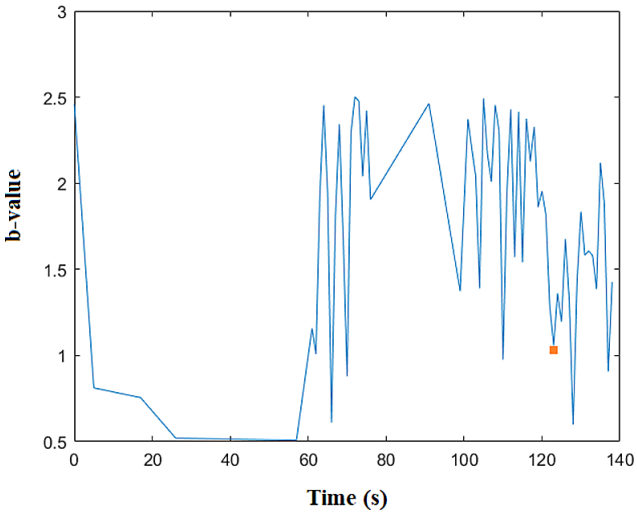

Figure 30: Variations of b-value with time for the sample QP2

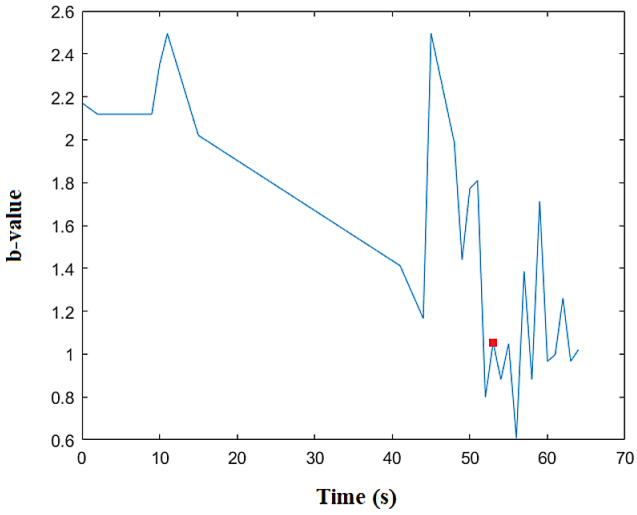

Figure 32: Variations of b-value with time for the sample QP4

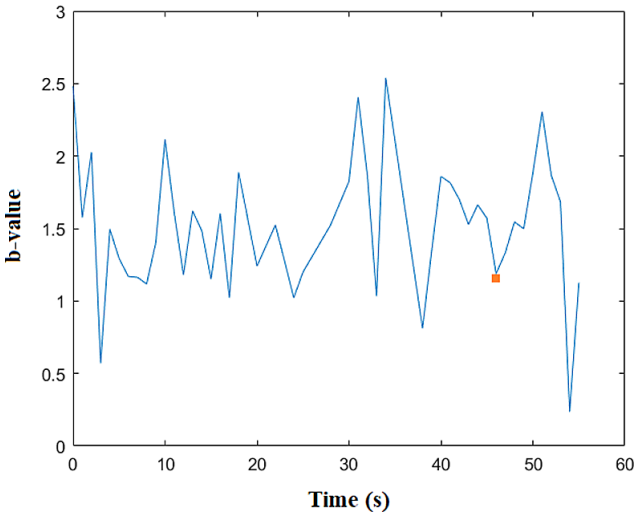

Figure 31: Variations of b-value with time for the sample QP3

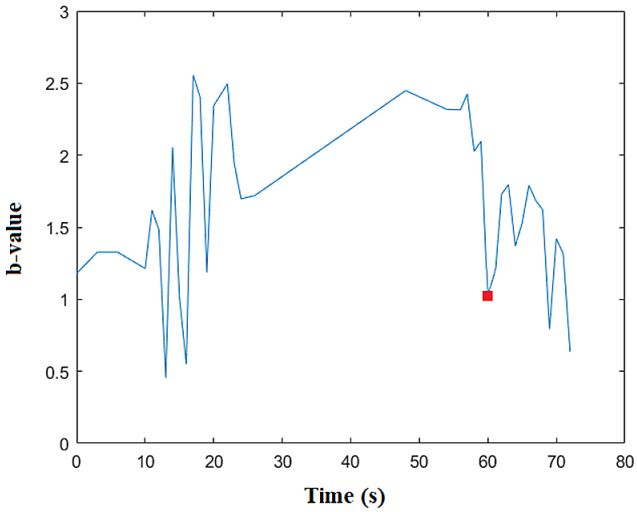

Figure 33: Variations of b-value with time for the sample QP5

QP3, respectively. In these figures, the horizontal axis denotes time (*i.e.* the hit length) while the vertical axis is the frequency. The colour code shown in the **Figures 16** to **18** shows the intensity of the corresponding peak frequency. As is evident in **Figure 16**, in the hit no. 342 for the sample QP1, the maximum intensity occurred at a frequency of 18 kHz. Moreover, **Figure 17** and **18** show that the peak frequencies for the hits no. 497 and 802 of the samples QP2 and QP3 are 31 kHz and 22 kHz, respectively.

The frequency range of acoustic emission signals varies for different materials and sources. For example, for metals it is between a few kilohertz to several megahertz, for composites it is between a few kilohertz to a few hundred kilohertz, and for rocks it is between a few hertz to a few hundred kilohertz (**Hou et al., 2021**). The peak frequency distribution provided for the acoustic emission signals of the phyllite specimens varies between 0 and 350 kHz. It is stated that high frequencies are associated with tensile cracks and low frequencies are associated with shear cracks (**Shengxiang et al., 2021**). As can be seen, due to the high frequencies in the Kaiser effect range, tensile cracks are the main source of the Kaiser effect.

Figures 19 through **23** show the obtained peak frequencies for all hits upon the acoustic emission tests on the samples QP1 through QP3, respectively. As the figures indicate, an increase occurs in the number of hits with relatively high (> 200 kHz) peak frequencies within the range of the Kaiser effect. The peak frequency is high at the time of the Kaiser effect. This is related to the increase in crack propagation rate, which means that a higher peak frequency reflects a higher crack propagation rate. It is stated that high frequencies are associated with tensile cracks and low frequencies are associated with shear cracks (**Bak et al., 2013; Shengxiang et al., 2021**). In this research, high frequency at the time of the Kaiser effect shows that the effect is sourced from tensile cracks. Finally, the increase in the number of hits within the range of the Kaiser effect reflects an increase

Table 3: Results of investigating the mechanism of the Kaiser effect

Sample Name	Time of Kaiser Effect (s)	Energy in Kaiser Point (eu)	RA/AF Ratio	*b*-value
QP1	31.3	3.5×10^{7}	0.04	1.15
QP2	123.6	9.73×10^{7}	0.06	1.05
QP3	46.5	7.37×10^{7}	0.05	1.10
QP4	52.8	2.23×10^{3}	0.02	1.04
QP5	60	4.5×10^{3}	0.04	1.09

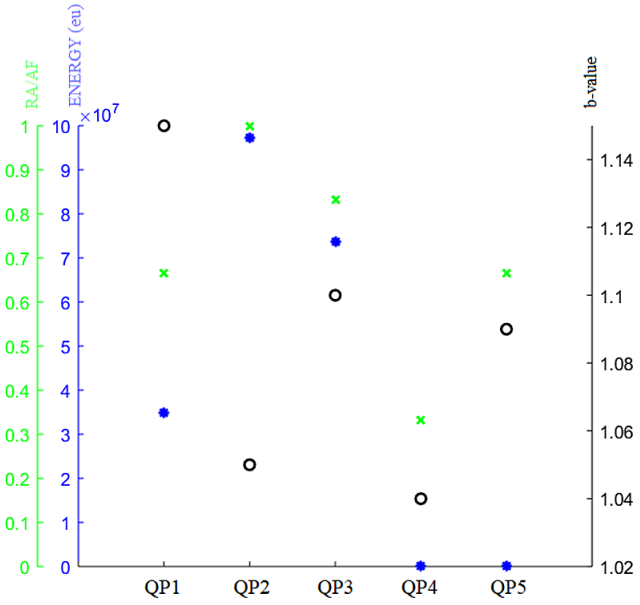

Figure 34: Values obtained from different parameters at the Kaiser effect point for the tested samples

in the number of cracks in that range (**Moradian et al., 2016**).

The energy level is an important parameter for investigating the mechanism of the Kaiser effect (**Sause, 2016**). In this research, the unit for energy level was eu. Developed by the Vallen Company, an eu is equivalent to 10^{-12} J. the energy level is directly related to the intensity of crack formation in the sample (**Bak et al., 2013**). As shown in **Figures 24** through **28**, the energy level increased significantly at the time of the Kaiser effect, reflecting the high intensity of crack formation at this point, as explained earlier.

The value of the *b*-value parameter is examined to analyze and study the mechanism of occurrence of the Kaiser effect. Regarding the *b*-value, the higher this parameter, the smaller the magnitude of the acoustic emission, and vice versa (**Ohtsu and Tomoda, 2007**). Moreover, previous studies have shown that *b*-values below 1 signify large failure events in the samples (**Sagar et al., 2012**). **Figures 29** through **33** indicate the *b*-values for the samples QP1 through QP5, respectively. As is evident in **Figure 29**, at the time of the Kaiser effect, the *b*-value is 1.15. As detailed previously, the fact that this value exceeds 1 show the occurrence of microcracks, while the relatively low value of this parameter reflects the largeness of the associated acoustic emission and indicates large cracks that are visible to the naked eye. As can be seen, the *b*-value related to the failure point of the sample, which includes large cracks, is less than one. Based on **Figures 30** through **33**, the *b*-values are 1.05, 1.10, 1.04 and 1.09 at the time of the Kaiser effect, respectively. Therefore, the corresponding samples (*i.e.* QP2 through QP5) suffer from microcrack-induced acoustic emissions of high intensity. **Table 3** summarizes the results of investigating the mechanism of the Kaiser effect.

Figure 34 shows the values obtained for different parameters at the Kaiser effect point. As shown in **Figure 34**, the sample QP1 has low energy, RA/AF, and higher *b*-value in the Kaiser effect. The sample QP2 has high energy, RA/AF and low *b*-value, and the sample QP3 has moderate values in all parameters. The sample QP4 has lower magnitude for all parameters than the others and the sample QP5 has low energy and a moderate *b*-value and RA/AF ratio.

4. Conclusions

The following conclusions were drawn based on the acoustic emission tests performed on three samples of phyllite rock.

Different rocks exhibit different mechanisms of the Kaiser effect with different sources. Based on the acoustic emission parameters obtained for the phyllites under the Brazilian tensile tests, the Kaiser effect was found to be a result of tensile stresses.

Regarding the obtained values of peak frequency, it was discovered that the rate of crack propagation is higher in the range of the Kaiser effect. In addition, the relatively high peak frequencies confirmed the tensile nature of the source of Kaiser effect.

The increase in the energy level at the Kaiser effect point show that the crack formation intensity is higher at this point rather than other points. The increase in the number of hits in the vicinity of the Kaiser effect point indicated the higher count of cracks formed in this region rather than other ranges.

The low *b*-value at the Kaiser effect point showed that the acoustic emission intensity is higher at the Kaiser effect point. However, the obtained *b*-values were above 1, indicating that the acoustic emission was sourced from microcracks.

References

Aki, K. (1965): Maximum likelihood estimate of b in the formula log N= a-bM and its confidence limits. Bulletin of the Earthquake Research Institute, University of Tokyo, 43, 2, 237-239.

Bak, K.M., KalaiChelvan, K., Vijayaraghavan, G., and Sridhar, B. (2013): Acoustic emission wavelet transform on adhesively bonded single-lap joints of composite laminate during tensile test. Journal of Reinforced Plastics and Composites, 32, 2, 87-95. doi:10.1177/0731684412459249

Beltyukov, N. (2021): Studying the Kaiser Effect During Modeling of Rock Loading Conditions Using the NX-borehole Jack. Journal of Physics, Conference Series, 1945, 1. doi:10.1088/1742-6596/1945/1/012023

Briševac, Z., and Kujundžić, T. Models to estimate Brazilian indirect tensile strength of limestone in saturated state. Rudarsko-geološko-naftni zbornik. 2016, 31, 59-67. doi: 10.17794/rgn.2016.2.5

Briševac, Z., Kujundžić, T., and Čajić, S. Current cognition of rock tensile strength testing by Brazilian test. Rudarsko-geološko-naftni zbornik. 2015, 30, 101-128. doi:10.17794/rgn.2015.2.2

Cao, A., Jing, G., Ding, Y., and Liu, S. (2019): Mining-induced static and dynamic loading rate effect on rock damage and acoustic emission characteristic under uniaxial compression. Safety Science, 116, 86-96. doi:10.1016/j.ssci.2019.03.003

Carneiro, F.L.L.B. (1943), "A new method to determine the tensile strength of concrete" Proceedings of the 5th meeting of the Brazilian Association for Technical Rules (''Associac ¸a˜o Brasileire de Normas Te´cnicas—ABNT''), 3d. Section, pp. 126-129. (in Portuguese)

Chen, Y., Irfan, M., and Song, C. (2018): Verification of the Kaiser effect in rocks under tensile stress: experiment using the Brazilian test. International Journal of Geomechanics, 18, 7, pp.7. doi:10.1061/(ASCE)GM.1943-5622.0001181

Chen, Z., Xu, L., and Shang, Y. (2021): Influence of joint angle on the acoustic emission evolution characteristics and energy dissipation rule of rock mass. Geotechnical and Geological Engineering, 39, 2, 1621-1635. doi:10.1007/s10706-020-01581-2

Fu, X., Ban, Y., Xie, Q., Abdullah, R.A., and Duan, J. (2021): Time Delay Mechanism of the Kaiser Effect in Sandstone Under Uniaxial Compressive Stress Conditions. Rock Mechanics and Rock Engineering, 54, 3, 1091-1108. doi: 10.1007/s00603-020-02310-0

Haldar, S.K. (2020): Introduction to mineralogy and petrology. Elsevier. 436 p. doi: 10.1016/C2019-0-00625-5

Hardy, H.R. (2003): Acoustic Emission/Microseismic Activity (Vol. 1). A.A. Balkema, Lisse, Netherlands.

Hardy, H.R. and Leighton, F.W. (1984): Acoustic emission/microseismic activity in geologic structures and materials. Trans Tech Publications. Limited, Zurich, Switzerland.

Hou, Z., Li, C., Song, Z., Xiao, Y., Qiao, C., and Wang, Y. (2021): Investigation on Acoustic Emission Kaiser Effect and Frequency Spectrum Characteristics of Rock Joints Subjected to Multilevel Cyclic Shear Loads. Geofluids. pp. 21. doi:10.1155/2021/5569525

Hsieh, A., Dight, P., and Dyskin, A. (2015): The rock stress memory unrecoverable by the Kaiser effect method. International Journal of Rock Mechanics and Mining Sciences, 75, 190-195. doi:10.1016/j.ijrmms.2015.01.006

ISRM (1978): Suggested methods for determining tensile strength of rock materials. International Journal of Rock Mechanics and Mining Sciences and Geomechanics Abstracts, 15, 3, 99–103. doi:10.1016/0148-9062(78)90003-7

Kaiser, E.J. (1950): An Investigation into the Occurrence of Noises in Tensile Tests or a Study of Acoustic Phenomena in Tensile Tests, [Ph.D thesis], Dissertation Technische Hochschule Munchen, Munich, Germany.

Kazareni, T. (2013): A discontinuum-based model to simulate compressive and tensile failure in sedimentary rock, Journal of Rock Mechanics and Geotechnical Engineering, 5, 378–388. doi:10.1016/j.jrmge.2013.07.002

Kent, L., Bigby, D., Coggan, J., and Chilton, J. (2002), "Comparison of acoustic emission and stress measurement results to evaluate the application of the Kaiser effect for stress determination in underground mines" Proceedings of the 21st International Conference on ground control in mining, Morgantown, West Virgina, USA, pp. 270–277.

Kharghani, M., Goshtasbi, K., Nikkah, M., and Ahangari, K. (2021): Investigation of the Kaiser effect in anisotropic rocks with different angles by acoustic emission method. Applied Acoustics, 175, p. 107831. doi:10.1016/j.apacoust.2020.107831

Khoshouei, M., and Bagherpour, R. Application of Acoustic Emission (AE) in mining and earth sciences: a review. Rudarsko-geološko-naftni zbornik. 2019, 34, 4. doi: 10.17794/rgn.2019.4.3

Khoshouei, M., Bagherpour, R., Jalalian, M.H., and Yari, M. Investigating the acoustic signs of different rock types based on the values of acoustic signal RMS. Rudarsko-geološko-naftni zbornik. 2020, 35, 3. doi:10.17794/rgn.2020.3.3

King, T., Benson, P., De Siena, L., and Vinciguerra, S. (2021): Acoustic emission waveform picking with time delay neural networks during rock deformation laboratory experiments. Seismological Society of America, 92, 2A, 923-932. doi:10.1785/0220200188

Kunpeng, L., Wuzhou, Z., Xiaotong, X., Yu, Z., Daoyong, W., and Xingyuan, J. (2021): Kaiser effect of cracked sandstone under different loading rotating angles. Arabian Journal of Geosciences, 14, 18, 1-11. doi:10.1007/s12517-021-08283-w

Kyriazopoulos, A., Stavrakas, I., Anastasiadis, C., and Triantis, D. (2015): Analysis of acoustic emissions from cement beams when applying three-point bending with different loading rates. In: Rudas, I.J. (ed.): RECENT RESEARCHES in MECHANICAL and TRANSPORTATION SYSTEMS, 57-63.

Lajtai, E. (1980): Tensile strength and its anisotropy measured by point and line-loading of sandstone. Engineering geology, 15, 163-171. doi:10.1016/0013-7952(80)90032-0

Lavrov, A. (2001): Kaiser effect observation in brittle rock cyclically loaded with different loading rates. Mechanics of

materials, 33, 11, 669-677. doi:10.1016/S0167-6636(01)00081-3

Lavrov, A., Vervoort, A., Wevers, M. and Napier, J.A.L. (2002): Experimental and numerical study of the Kaiser effect in cyclic Brazilian tests with disk rotation. International Journal of Rock Mechanics and Mining Sciences, 39, 3, 287–302. doi:10.1016/S1365-1609(02)00038-2

Lehtonen, A., Cosgrove, J., Hudson, J., and Johansson, E. (2012): An examination of in situ rock stress estimation using the Kaiser effect. Engineering Geology, 124, 24-37. doi:10.1016/j.enggeo.2011.09.012

Li, D. and Wong, L.N.Y. (2013): The Brazilian disc test for rock mechanics applications: review and new insights. Rock Mechanics and Rock Engineering, 46, 2, 269-287. doi:10.1007/s00603-012-0257-7

Li, Y., Yang, Y., Liu, J., and Zhao, X. (2010): Experimental and theoretical analysis on the procedure for estimating geostresses by the Kaiser effect. International Journal of Minerals, Metallurgy, and Materials, 17, 5, 514-518. doi:10.1016/j.ijsolstr.2017.01.014

Li, Z., and Xu, R. (2021): An early-warning method for rock failure based on Hurst exponent in acoustic emission/microseismic activity monitoring. Bulletin of Engineering Geology and the Environment, 1-15. doi:10.1007/s10064-021-02446-5

Liu, H. (2000): Acoustic emission and crack development in rocks, University of Hong Kong, Pokfulam, Hong Kong. doi:10.5353/th_b3124206

Main, I. G., Meredith, P.G., and Jones, C. (1989): A reinterpretation of the precursory seismic b-value anomaly from fracture mechanics. Geophysical Journal International, 96, 1, 131-138.

Meng, Q., Chen, Y., Zhang, M., Han, L., Pu, H., and Liu, J. (2019): On the Kaiser effect of rock under cyclic loading and unloading conditions: insights from acoustic emission monitoring. Energies, 12, 17, 32-55. doi:10.3390/en12173255

Montoto, M., and Hardy, H.R. (1991), "Kaiser effect in intact rock: current status as a feasible means of evaluating thermal and mechanical loading" Proceedings of 7th International Congress on Rock Mechanics, Aachen/Deutschland, pp. 569–572.

Moradian, Z., Einstein, H.H., and Ballivy, G. (2016): Detection of cracking levels in brittle rocks by parametric analysis of the acoustic emission signals. Rock Mechanics and Rock Engineering, 49, 3, 785-800. doi:10.1007/s00603-015-0775-1

Newman, D. and Bennett, D. (1990): The effect of specimen size and stress rate for the Brazilian test—a statistical analysis. Rock Mechanics and Rock Engineering, 23, 123-134. doi:10.1007/BF01020397

Nikkhah, M., Ahmadi, M., and Ghazvinian, A. (2011), "Application of pattern recognition analysis of rock acoustic emission for determination of Kaiser Effect" Proceedings of 12th International Congress on Rock Mechanics, China. 765-769.

Ohtsu, M., and Tomoda, Y. (2007): Corrosion process in reinforced concrete identified by acoustic emission. Materials transactions, 48, 6, 1184-1189. doi: 10.2320/matertrans.I-MRA2007844

Pandey, P. and Singh, D. (1986): Deformation of a rock in different tensile tests. Engineering geology, 22, 281-292. doi:10.1016/0013-7952(86)90029-3

Rao, M., and Lakshmi, K.P. (2005): Analysis of b-value and improved b-value of acoustic emissions accompanying rock fracture. Current science, 89, 9, 1577-1582.

Sagar, R.V., Prasad, B.R., and Kumar, S.S. (2012): An experimental study on cracking evolution in concrete and cement mortar by the b-value analysis of acoustic emission technique. Cement and Concrete Research, 42, 8, 1094-1104. doi:10.1016/j.cemconres.2012.05.003

Sause, M.G. (2016): In situ monitoring of fiber-reinforced composites: theory, basic concepts, methods, and applications (Vol. 242). Springer. Berlin, Germany, 633 p. doi:10.1007/978-3-319-30954-5

Seto, M., Nag, D., and Vutukuri, V. (1996), "Evaluation of rock mass damage using acoustic emission technique in the laboratory. In Rock Fragmentation by Blasting" Proceedings of the 5th International Symposium on Rock Fragmentation by Blasting. Montreal, Quebec, Canada, pp. 139–145.

Seto, M., and Villaescusa, E. (1999), "In situ stress determination by acoustic emission techniques from McArthur River mine cores" Proceedings of 8th Australia New Zealand Conference on Geomechanics, Hobart, Australia, pp. 929-934.

Shengxiang, L., Qin, X., Xiling, L., Xibing, L., Yu, L., and Daolong, C. (2021): Study on the acoustic emission characteristics of different rock types and its fracture mechanism in Brazilian splitting test. Frontiers in Physics, 9. doi: 10.3389/fphy.2021.591651

Shiotani, T. (2001): Application of the AE Improved b-Value to Quantiative Evaluation of Fracture Process in Concrete-Materials. Journal of Acoustic Emission, 19, 118-133. doi: 10.3389/fphy.2021.591651

Tuncay, E., and Ulusay, R. (2008): Relation between Kaiser effect levels and pre-stresses applied in the laboratory. International Journal of Rock Mechanics and Mining Sciences, 45, 4, 524-537. doi:10.1016/j.ijrmms.2007.07.013

Wang, Q.Z., Jia, X.M., Kou, S.Q., Zhang, Z.X. and Lindqvist P.A. (2004): The flattened Brazilian disc specimen used for testing elastic modulus, tensile strength and fracture toughness of brittle rocks: analytical and numerical results. International Journal of Rock Mechanics and Mining Sciences, 41, 2, 245–253. doi:10.1016/S1365-1609(03)00093-5

Wang, Y., Deng, H., Deng, Y., Chen, K., and He, J. (2021): Study on crack dynamic evolution and damage-fracture mechanism of rock with pre-existing cracks based on acoustic emission location. Journal of Petroleum Science and Engineering, 201, 7, 108420. doi:10.1016/j.petrol.2021.108420

Yuan, R., and Li, Y. (2008): Theoretical and experimental analysis on the mechanism of the Kaiser effect of acoustic emission in brittle rocks. Journal of University of Science and Technology Beijing, Mineral, Metallurgy, Material, 15, 1, 1-4. doi:10.1016/S1005-8850(08)60001-8

Zadsar, H., Cheraghi Seifabad, M., and Ahmadi, M. An investigation into fracture toughness and mechanisms in anisotropic rocks using the Acoustic Emission method. Rudarsko-geološko-naftni zbornik. 2020, 35, 2, 15-21. doi:10.17794/rgn.2020.2.2

Zhou, Z., Zhou, J., Zhao, Y., Chen, L., and Li, C. (2021): Microscopic Failure Mechanism Analysis of Rock Under Dynamic Brazilian Test Based on Acoustic Emission and Moment Tensor Simulation. Frontiers in Physics, 8, 1-14. doi:10.3389/fphy.2020.592483

SAŽETAK

Mehanizam Kaiserova efekta u filitu pri vlačnome opterećenju neizravnim mjerenjem

In situ određivanje naprezanja, među ostalim, služi kao važan korak u projektiranju i izradi građevinskih i rudarskih projekata. Konvencionalne *in situ* metode mjerenja naprezanja vremenski su i troškovno zahtjevne. Stoga istraživači sve više razmatraju primjenu jeftinih, ali brzih metodologija za procjenu *in situ* naprezanja. Metoda akustične emisije koja se temelji na Kaiserovu efektu jedan je od takvih novih pristupa u procjeni *in situ* naprezanja. Ne samo točka u kojoj se Kaiserov efekt javlja, nego i mehanizam Kaiserova efekta od iznimne je važnosti. U ovome su istraživanju provedena ispitivanja akustičke emisije na uzorcima filitnih stijena pri ispitivanju vlačne čvrstoće stijena uporabom brazilskoga testa kako bi se prikupili različiti akustički podatci uključujući amplitudu, vrijeme porasta, broj, trajanje i energiju. Potom je na temelju prikupljenih podataka o akustičkim parametrima određena točka Kaiserova efekta te je ispitan mehanizam njezina nastanka. Osim toga, usvojene su matematičke transformacije za transformaciju akustičkoga signala iz vremenske domene u frekvencijsko područje, gdje je analizirana vršna frekvencija. Rezultati analize omjera RA/AF pokazali su da je akustička emisija nastala iz vlačnih mikropukotina. Štoviše, visoka razina energije upućuje na visok intenzitet stvaranja pukotina u točki Kaiserova efekta. Velik broj primljenih impulsa pokazao je da se broj novonastalih pukotina naglo povećava unutar raspona Kaiserova efekta. Osim toga, dobivena visoka vrijednost vršne frekvencije implicira da je brzina širenja pukotine visoka u točki Kaiserova efekta.

Ključne riječi:
akustička emisija, Kaiserov efekt, vršna frekvencija, filit, brazilski test vlačne čvrstoće

Author's contribution

Mohammadmahdi Dinmohammadpour (1) (PhD candidate) carried out the experiments and provided analyses, validation, writing, presentation and interpretation of the results. **Majid Nikkhah (2)** (Assistant Professor at the Faculty of Engineering) designed the experiments and contributed to the methodology and the interpretation of results. **Kamran Goshtasbi (3)** (Professor at the Faculty of Engineering) provided the conceptualization. **Kaveh Ahangari (4)** (Associate Professor at the Faculty of Engineering) performed the investigation of the results.